LETTERS
https://doi.org/10.1038/s41558-019-0682-7

nature climate change

Persistent Quaternary climate refugia are hospices for biodiversity in the Anthropocene

Stuart C. Brown[1*], Tom M. L. Wigley[1,2], Bette L. Otto-Bliesner[2], Carsten Rahbek[3] and Damien A. Fordham[1,3*]

Climate stability leads to high levels of speciation and reduced extinction rates, shaping species richness patterns[1–3]. Hotspots of species diversity often overlap with regions that experienced stable temperatures and, perhaps, variable rates of precipitation during the late Quaternary[4,5]. These hotspots potentially harbour many species with low vagility and small geographical ranges[6], making them more vulnerable to future ecoclimatic change[4,7,8]. By comparing global and regional patterns of climate stability during short periods of unusually large and widespread climate changes since the Last Glacial Maximum with twenty-first-century patterns, we show that human-driven climate change will disproportionally affect biodiversity in late Quaternary climate refugia, ultimately affecting the species, communities and ecosystems that are most vulnerable to climate change. Moreover, future changes in absolute temperature will probably erode the mechanisms that are theorized to sustain biodiversity hotspots across time. These impending shifts from stable to unstable temperatures—projected for the majority of the world's biodiversity regions—threaten to reduce the size and extent of important climatic safe havens for diversity. Where climate refugia are forecast to persist until the end of this century, temperatures in these refuges are likely to exceed the acclimation capacity of many species, making them short-term hospices for biodiversity at best[7–9].

Long-term stability of the mean climate state is hypothesized to be a crucial factor that is responsible for spatio-temporal variations in biodiversity[1–9]. Stable temperatures and, to a lesser extent, their interaction with precipitation rates have been linked to differences in species richness and rates of endemism[10]. Minor changes (at most) in mean climate states, particularly for temperature, are generally thought to be necessary to make in situ persistence possible for species that have small geographical ranges[7]. Low-range movement and high local survival results in species becoming specialized to local abiotic and biotic conditions and potentially more vulnerable to larger changes in temperature[11]. By contrast, unstable mean climate states (that is, large temporal variability in temperature) often require species to have large geographical ranges and high dispersal capabilities to reduce extinction risk. Furthermore, species in relatively stable climate regions tend to have higher genetic variation among individuals[12] as a result of lower local extinction rates and a more complex population structure[2], providing an increased propensity for evolutionary change in response to new environmental conditions[13].

To test the theory that the stability of regional climates on century to millennial timescales determines local diversity, with centres of endemism typically occurring where past climate fluctuations have been relatively rare and low in magnitude[4–6,14], we need information on patterns of past climate change down to at least subcentennial timescales[15]. However, global climate simulations for the late Quaternary have, until the last decade, only been available at widely spaced (usually >1,000 yr) climate snapshots[15]. Since regional climates have changed considerably across decades and centuries during glacial–interglacial cycles (probably causing rapid regional replacement of biota[16]), a more temporally detailed picture of past changes is required to fully assess the role of climate stability on geographical patterns of old and young species.

To this end we use atmosphere–ocean general circulation models (AOGCMs; Supplementary Table 1) to compare continuous global climate simulations of annual means of the daily temperature and precipitation, calculated for the period from the Last Glacial Maximum (LGM; 21,000 yr BP) until large-scale industrialization (100 yr BP; that is, AD 1850), as well for the twenty-first century (AD 2010–2100). We characterize climate stability on timescales that affect evolutionary processes and extinction rates[15] for periods of rapid global mean temperature change (see Methods) and show that anthropogenic warming this century will (1) erode biologically important latitudinal gradients in temperature stability, and (2) destabilize and potentially eliminate putative late Quaternary climate refugia, most probably having a strong negative effect on hotspots of biodiversity.

To do this we characterize regional climate stability using two novel and complementary methods. We first used modelled global mean temperature data to select periods of rapid climate change at a near-century timescale (see Methods). For these periods we then calculated the magnitudes of the near-century trends and the s.d. of the residuals about these trends for each grid cell ($n = 10{,}368$) and determined the quartiles for temperature and precipitation across grid-cells[17]. We did this for land ($n = 4{,}066$) and ocean ($n = 6{,}302$) realms separately. The climate was then classified according to six levels of climate stability, ranging from stable to unstable[17] for any given grid cell and time point (see Methods).

Although these categorical data allow regions of different climate states to be defined and illustrated, such data are less useful for quantifying change. We employ a second definition to address this where stable climates are defined using the signal-to-noise ratio (SNR), defined as the near-century trend divided by the s.d. of residuals about the trend, where low SNR values signify stable climates (small magnitudes of change, given interannual variability) and high SNR values denote unstable climate conditions (large magnitudes of change, given interannual variability).

[1]The Environment Institute and School of Biological Sciences, University of Adelaide, Adelaide, South Australia, Australia. [2]Climate and Global Dynamics Laboratory, National Center for Atmospheric Research, Boulder, CO, USA. [3]Center for Macroecology, Evolution, and Climate, GLOBE Institute, University of Copenhagen, Copenhagen, Denmark. *e-mail: s.brown@adelaide.edu.au; damien.fordham@adelaide.edu.au

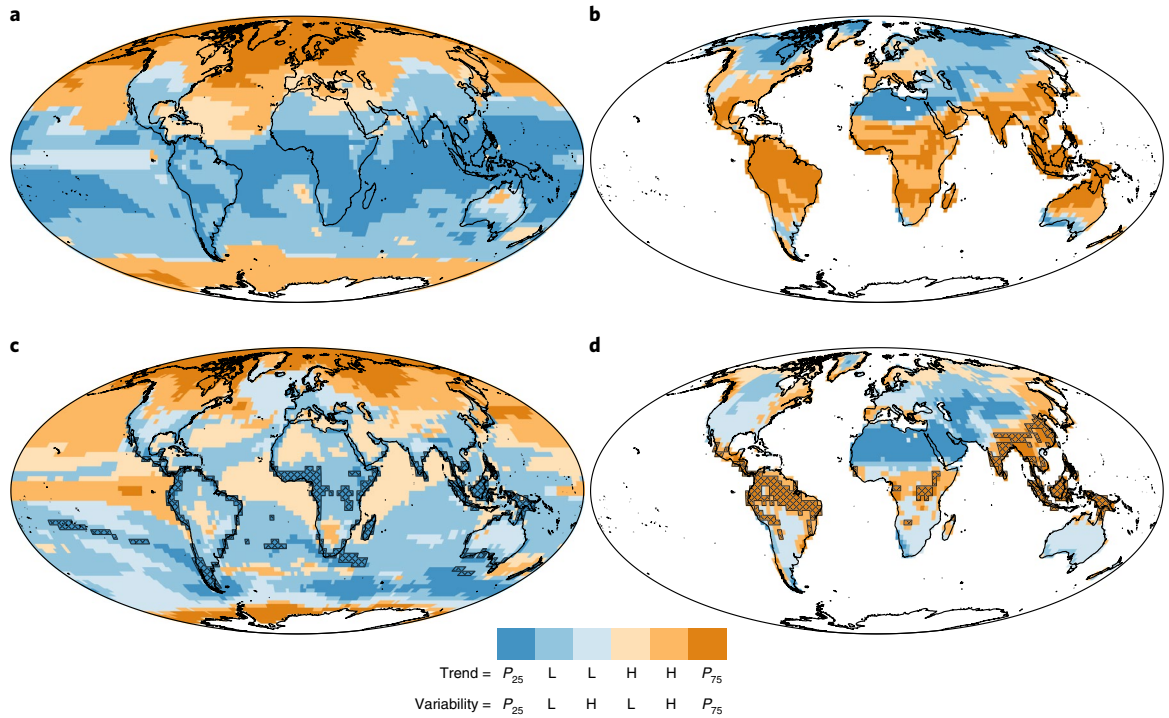

Fig. 1 | Classified median trend and variability during periods of rapid change in global mean temperature. a–d, Panels show the past (**a**,**b**) and future under RCP 8.5 (**c**,**d**) for surface temperature (**a**,**c**) and precipitation (**b**,**d**). The six classes map the median trend and variability (s.d. of residuals from the trend) calculated separately for land and ocean: ≤25th (P_{25}); >25th and ≤50th (low–low); ≤50th for trend and ≥50th for variability (low–high); >50th for trend and ≤50th for variability (high–low); >50th and ≤75th (high–high); >75th (P_{75}). The hatched overlays in **c** and **d** show climatic conditions that are considered as either stable (≤P_{25}, surface temperature) or unstable (≥P_{75}, precipitation) at a global scale in both the past and future. See Extended Data Fig. 1 for results for RCP 4.5. H, high; L, low.

Our palaeoclimate simulations show a latitudinal gradient in temperature stability since the LGM (Fig. 1a), in accordance with the climate stability hypothesis for the geographic pattern of global diversity[18]. Greater than 58% of tropical terrestrial and marine environments have experienced regional-scale temperatures that were relatively 'stable' over the past ~21,000 yr; compared to <8% outside of the tropics. In tropical terrestrial environments, areas with long-term 'stable' temperatures coincide with areas that experienced 'unstable' precipitation conditions over the past ~21,000 yr (Fig. 1b), emphasizing support for a hypothesized connection between variable precipitation and present-day patterns of biodiversity[4,5,10]. We show that 48% of the area of prominent terrestrial biodiversity hotspots[19] intersect areas characterized by late Quaternary 'stable' temperature and 'unstable' precipitation conditions (Fig. 2a).

A proposed mechanistic role of unstable precipitation in maintaining species richness through the late Quaternary is based on field and theoretical studies showing that the species composition of communities is seldom in a state of equilibrium[20] and that disturbances brought about by, for example, variable spatio-temporal patterns of precipitation (and the resultant expansion and contraction of suitable habitat, droughts, floods and so on) can maintain high diversity[5,20]. Accordingly, stable ecoclimatic conditions allow older species to survive and new lineages to be generated in the face of large-scale climate oscillations, whereas intermediate levels of disturbance at local to regional scales maximize diversity[4]. Moreover, rainfall variability can directly promote opportunities for species co-existence through niche partitioning[21].

We use generalized additive models to show that there is a strong association between contemporary patterns of species richness and climate stability during periods of rapid global-scale climate change throughout the late Pleistocene and Holocene, as predicted by theory. Instability in precipitation and, more specifically, high interannual

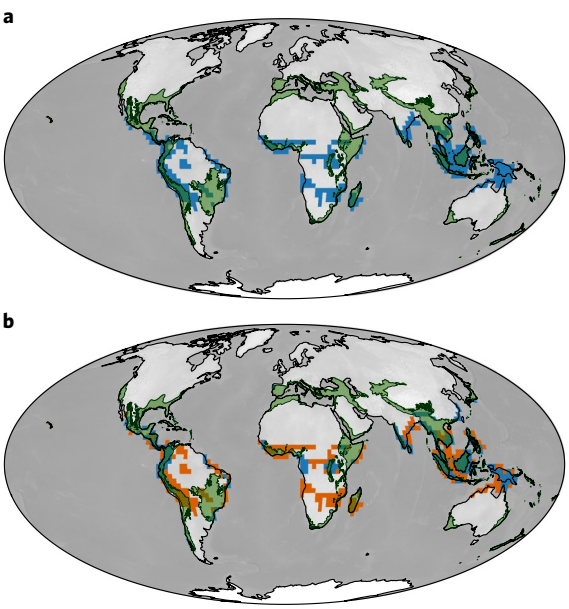

Fig. 2 | Areas of overlap in stable surface temperature (≤25th percentile) and unstable precipitation (≥75th percentile) conditions over land. a,**b**, The past (**a**) and the future under RCP 8.5 (**b**). Areas of overlap (regions where the climate conditions are hypothesized to drive higher contemporary species richness) are shown in blue. Areas in orange in **b**, show differences between the past and the future (that is, areas of overlap that are lost). The transparent green regions overlaid on the maps are biodiversity hotspots[19]. See Extended Data Fig. 2 for the results for RCP 4.5.

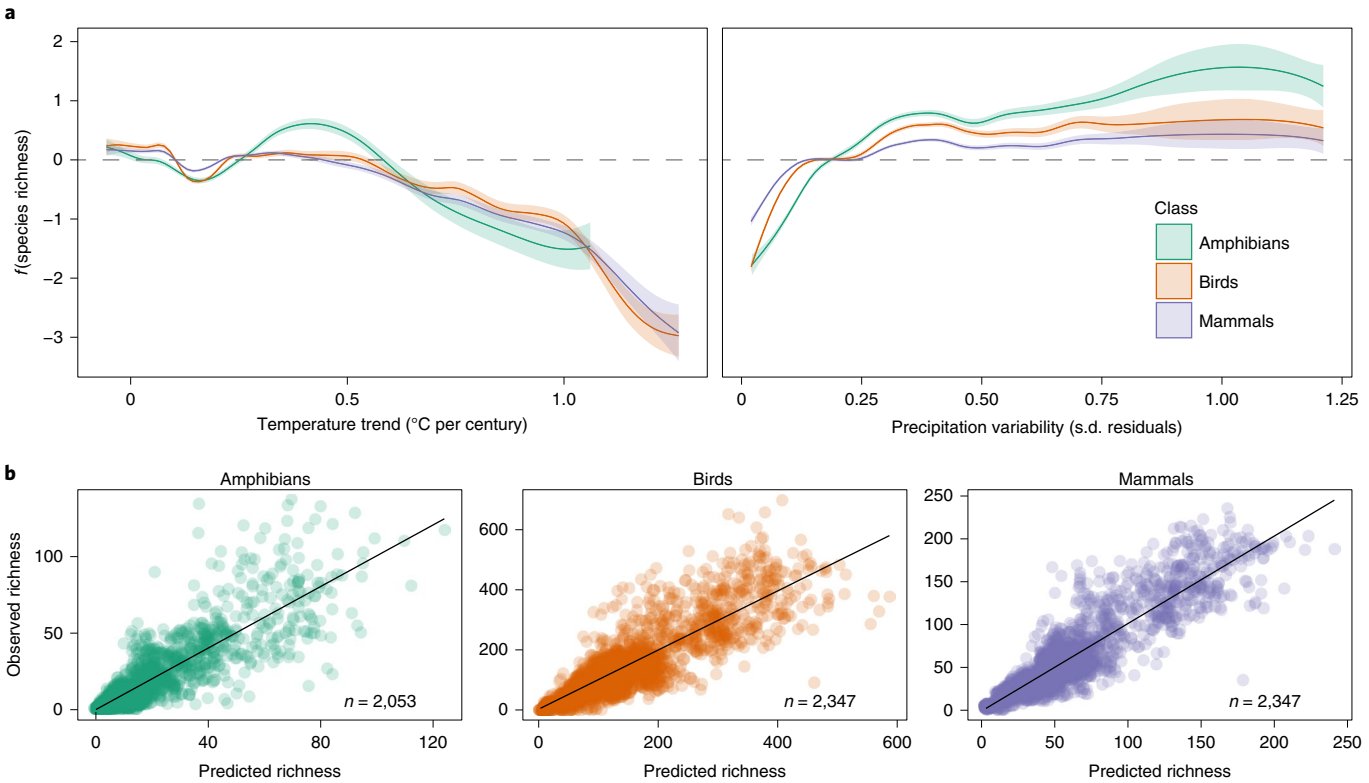

Fig. 3 | The relationship between contemporary species richness and past temperature trend and precipitation variability. a,**b**, The results of generalized additive models were used to investigate relationships between species richness and each of the following: climatic trends, variability and geographical location for three classes of animal (amphibians, birds and mammals). **a**, The smoothed functional effect (*f*) of temperature trend and precipitation variability on species richness. Trend and variability are median estimates for near centuries of rapid change in past global mean temperature (see Methods). Note that the *y* axes in **a** are on a logarithmic scale due to the log link used in the generalized additive model. The shaded envelopes show ±2 s.e. of the fit of the trend lines. **b**, Plots of observed and predicted species richness. The black lines are 1:1 lines.

variability in rainfall during near centuries of rapid change in global mean temperature, is positively associated with present-day global patterns of species richness for birds, mammals and amphibians (Fig. 3; Supplementary Table 2). Conversely, regions characterized by great temperature instability during these periods of rapid global-scale climate change typically have low species richness for the three classes. The best ranked models (according to the Akaike information criterion) for amphibians ($n = 2{,}053$ grid cells), birds ($n = 2{,}347$) and mammals ($n = 2{,}347$) modelled species richness as a function of trend in temperature, s.d. in rainfall and geographical position (richness $\approx f$ (temp. trend) $+ f$ (precip. var.) $+ f$ (lat.) $+ f$ (long.); where f is the smoothed functional effect), explaining 84%, 73% and 83% of the deviance, respectively (Supplementary Table 3). Although there was considerably less support for models that did not account for geographical position, they still explained between 56% and 70% of the deviance (Supplementary Table 3). Tenfold cross validation showed that these models of species richness were structurally robust and had good predictive skill, with low residual spatial autocorrelation (Supplementary Tables 2 and 3).

Warming during the twenty-first century is projected to occur at a much faster rate in many regions—with greater variability—than has been observed during the most rapid periods of climate change over the past 21,000 yr (Fig. 1, Supplementary Fig. 1). Globally, we estimate that >55% of land and ocean that exhibited stable temperature conditions in the past will become unstable by 2100 (Fig. 1c; Extended Data Fig. 1). The future is most ominous for tropical regions, with projected decreases of >75% in the area of stable temperature conditions. This loss is likely to be much larger over the oceans (~98% reduction) than the land (>37% reduction). Likewise, the area of terrestrial tropical regions with unstable precipitation conditions is projected to shrink by >37% (Fig. 1d), and areas with both stable temperatures and unstable precipitation by >42% (Fig. 2; Extended Data Fig. 2). As terrestrial species richness is negatively associated with the magnitude of near-century trends in grid-cell temperature (during periods of rapid change in global mean temperature) and positively associated with the variability of rainfall during these same periods, these changes can be expected to have strong direct (as well as indirect[22]) negative effects on diversity in tropical regions.

Although tropical latitudes are projected to continue to support a greater number of regions with stable temperatures in the near future than non-tropical latitudes (Fig. 1), species residing in these regions will be forced to contend with absolute temperatures that are novel from those experienced over the past 21,000 yr (Supplementary Fig. 1; a finding also shown elsewhere[23]), which are likely to be beyond the acclimation capacity of many species found there[24–26]. Regions with relatively stable temperature conditions, which we project to be few in number, are therefore unlikely to provide long-term safe havens for organisms to survive in during periods of unfavourable human-induced climate change.

Global-scale patterns of geographical variation in past and future climatic conditions based on the SNR are, in general, similar to those for our categorical measure of temperature stability, with the greatest change for temperature stability occurring in tropical latitudes (Fig. 4; Extended Data Fig. 3). The SNR estimates for precipitation indicate low levels of change in the stability of precipitation in all terrestrial regions, except for high northern latitudes (Fig. 4), which is somewhat at odds with our categorical approach, which projects a greater level of change between past and future spatial patterns

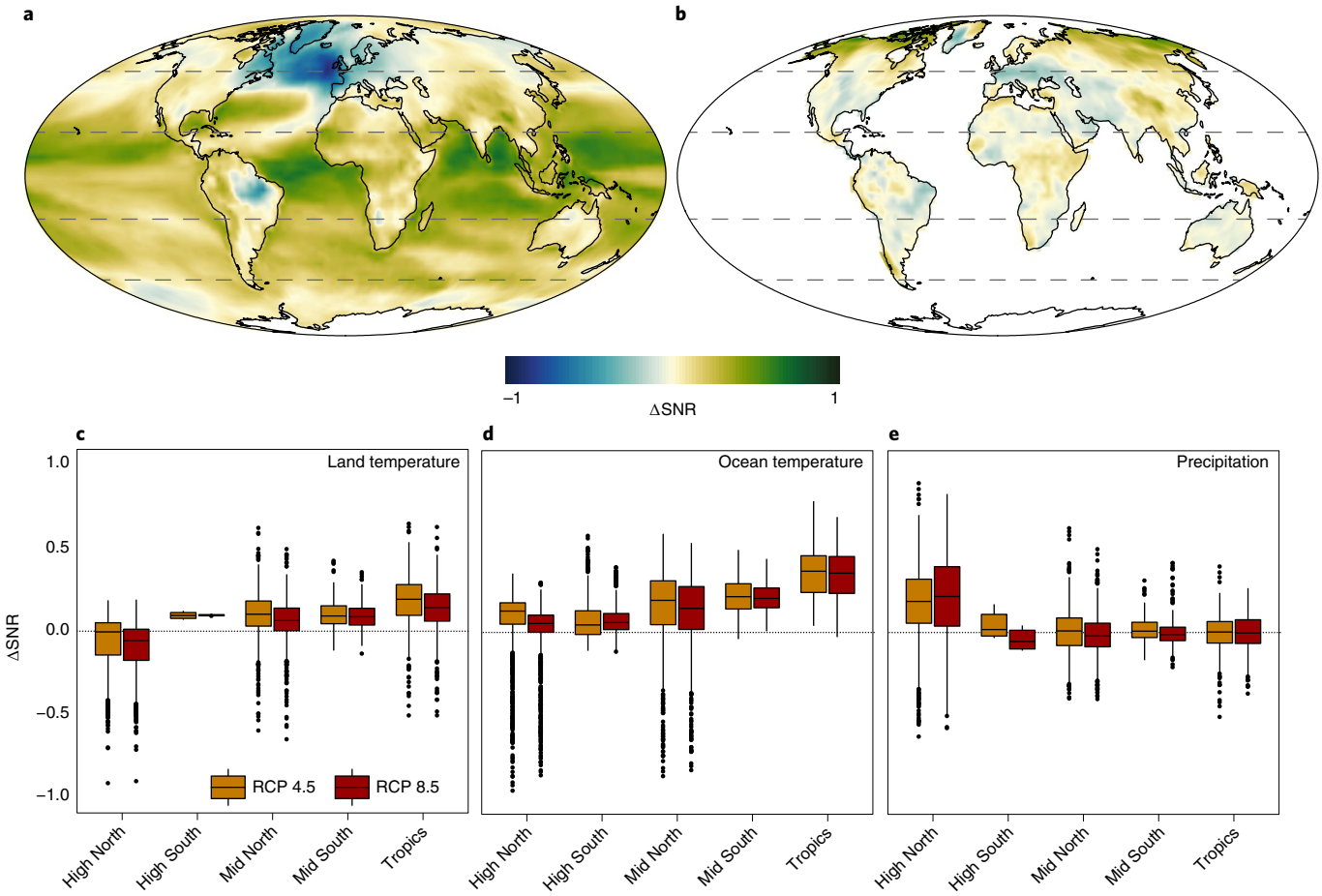

Fig. 4 | A comparison of past and future signal-to-noise ratios. a,**b**, Grid cell differences (ΔSNR) in the signal-to-noise ratio (SNR = trend/variability) for centuries of rapid change in the global mean temperature since 21,000 yr BP and RCP 8.5 calculated for air temperature (**a**) and precipitation (**b**). **c**–**e**, Boxplots that show the ΔSNR in land temperature (**c**), ocean temperature (sea surface temperature, **d**) and precipitation (**e**) for both RCPs 4.5 and 8.5 for five latitudinal bands: High North (50°N to 90°N), High South (90°S to 50°S), Mid North (20°N to 50°N), Mid South (50°S to 20°S) and the Tropics (20°S to 20°N). The ΔSNR in temperature over terrestrial and ocean realms are shown in **c** and **d**, respectively, whereas **e** shows the ΔSNR for precipitation over land. Positive ΔSNR values in **a**–**e** correspond to higher future SNRs whereas negative values correspond to higher past SNRs. Note that the SNR values were scaled globally between 0 and 1 before calculating ΔSNR. See Extended Data Fig. 3 for results for RCP 4.5 that correspond to panels **a** and **b**.

of rainfall instability; and recent forecasts of drying in subtropical regions in response to greenhouse gas emissions[27].

Projected increases in SNR for temperature were most pronounced for tropical oceans (Fig. 4a,d), particularly the Indo-Australian archipelago, which has extraordinary species richness and endemism[28]. These changes are likely to have severe negative impacts on species richness of corals and the marine life they support[25,29], causing associated human hardship for communities that depend on coral reefs for food, employment and income[30]. By contrast, the North Atlantic had a higher SNR for temperature in the past compared with what is being projected for the future (Fig. 4), potentially inducing strong selective pressures on organisms in this region, making these species potentially more resilient to future temperature changes, particularly if ocean biogeochemistry and ice-sheet dynamics remain relatively unchanged, which is likely only in the immediate future[30].

Similarly, terrestrial areas projected to experience the largest within-region shift in SNR for temperature are those with some of the highest concentrations of biodiversity. These include the Guinea-Congolian, Indo-Malayan and Madagascan Wallace zoogeographic regions (Fig. 5; Extended Data Fig. 4). Outside of the tropics, the zoogeographic regions of China, Japan and Tibet are projected to experience large magnitude shifts in temperature, exceeding even the most rapid rates of within-region change over the past 21,000 yr (Supplementary Figs. 2 and 3, Supplementary Tables 4 and 5). By contrast, high overlap between past and future SNR for precipitation in the future is expected for all of the zoogeographic regions except Tibet (Fig. 5); however there will be considerable changes in the distribution, location and median SNR precipitation values across some regions (Supplementary Tables 4 and 5), indicating a possible shift to novel precipitation SNR conditions in these areas. Stable temperature conditions during the late Quaternary, which probably permitted (at least in part) high rates of diversity (Fig. 3), particularly in tropical regions (Figs. 1 and 2), are therefore likely to be greatly reduced and, in some zoogeographic regions, entirely lost this century. This can be expected to negatively affect the persistence of local biodiversity[1–9].

The high temporal resolution of our data has demonstrated that conditions favourable for diversity and, more specifically, species richness are strongly influenced by centennial timescale climate fluctuations that have not often been considered (by necessity rather than design) in previous analyses of the effects of climate stability on diversity[15]. Although topography has often been regarded as a buffer to climatic extremes[6,14], our coarser resolution estimates of climate stability are relevant and important because continental-to-global patterns of contemporary patterns of diversity are most often attributed to regional differences in ecoclimatic stability[1,3].

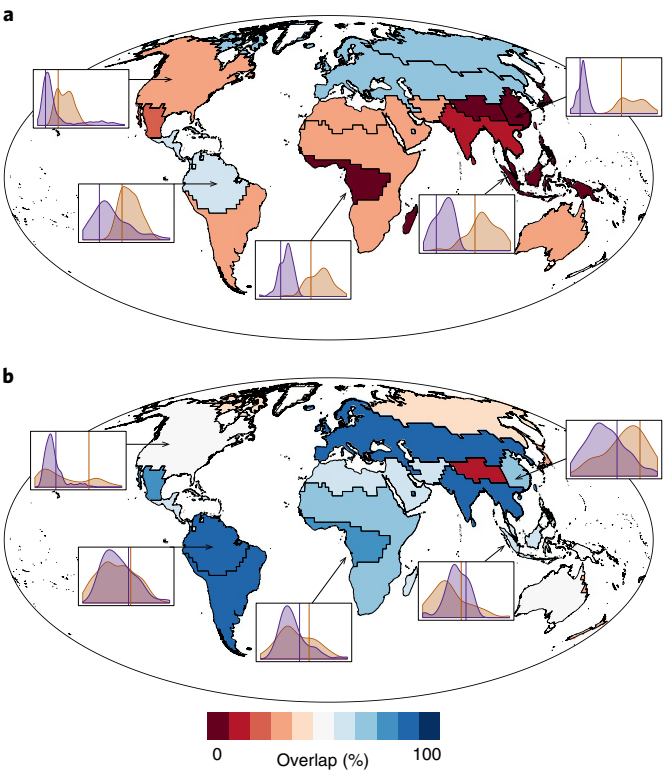

Fig. 5 | The regional changes in SNR for Wallace zoogeographic regions. **a**,**b**, The map of overlap between empirical kernel density estimates (KDE) for temperature SNR (**a**) and precipitation SNR (**b**), calculated during past rapid shifts in global mean temperature and under an RCP 8.5 scenario. The inset plots show selected KDEs (see Methods). A smaller KDE overlap indicates a greater shift away from past SNR (purple) conditions compared with future conditions (orange) for both temperature and precipitation. The vertical lines on the KDEs represent the 25th or 75th percentile for temperature and precipitation, respectively. Note that values were temporally scaled (from 0–1) between the past and future before calculating KDE. For results relating to RCP 4.5 see Extended Data Fig. 4.

The assumption we are making here is that macroscale changes in climate stability affect ecological and evolutionary processes that operate at finer (local environmental) spatial resolutions[12].

By showing that global and regional patterns of climate stability during the most recent deglaciation period differ strongly from future anthropogenically driven patterns, we provide new and compelling support that climate change this century is likely to disproportionally affect species in biodiversity hotspots and other tropical regions where diversity is greatest. Our results also highlight the importance of precipitation variability as well as stability in temperature during the late Quaternary as proximate drivers of terrestrial biodiversity patterns.

Online content

Any methods, additional references, Nature Research reporting summaries, source data, extended data, supplementary information, acknowledgements, peer review information; details of author contributions and competing interests; and statements of data and code availability are available at https://doi.org/10.1038/s41558-019-0682-7.

Received: 5 March 2019; Accepted: 12 December 2019;
Published online: 3 February 2020

References

1. Dynesius, M. & Jansson, R. Evolutionary consequences of changes in species' geographical distributions driven by Milankovitch climate oscillations. *Proc. Natl Acad. Sci. USA* **97**, 9115–9120 (2000).
2. Hewitt, G. The genetic legacy of the Quaternary ice ages. *Nature* **405**, 907–913 (2000).
3. Fine, P. V. A. Ecological and evolutionary drivers of geographic variation in species diversity. *Annu. Rev. Ecol. Evol. Syst.* **46**, 369–392 (2015).
4. Fjeldså, J. & Lovett, J. C. Geographical patterns of old and young species in African forest biota: the significance of specific montane areas as evolutionary centres. *Biodiv. Conserv.* **6**, 325–346 (1997).
5. Haffer, J. Speciation in amazonian forest birds. *Science* **165**, 131–137 (1969).
6. Fjeldså, J., Bowie, R. C. K. & Rahbek, C. The role of mountain ranges in the diversification of birds. *Annu. Rev. Ecol. Evol. Syst.* **43**, 249–265 (2012).
7. Jansson, R. Global patterns in endemism explained by past climatic change. *Proc. R. Soc. B* **270**, 583–590 (2003).
8. Sandel, B. et al. The influence of Late Quaternary climate-change velocity on species endemism. *Science* **334**, 660–664 (2011).
9. Harrison, S. & Noss, R. Endemism hotspots are linked to stable climatic refugia. *Ann. Bot.* **119**, 207–214 (2017).
10. Araújo, M. B. et al. Quaternary climate changes explain diversity among reptiles and amphibians. *Ecography* **31**, 8–15 (2008).
11. Dalsgaard, B. et al. Specialization in plant-hummingbird networks is associated with species richness, contemporary precipitation and Quaternary climate-change velocity. *PLoS ONE* **6**, e25891 (2011).
12. Carnaval, A. C., Hickerson, M. J., Haddad, C. F., Rodrigues, M. T. & Moritz, C. Stability predicts genetic diversity in the Brazilian Atlantic forest hotspot. *Science* **323**, 785–789 (2009).
13. Hughes, A. R., Inouye, B. D., Johnson, M. T., Underwood, N. & Vellend, M. Ecological consequences of genetic diversity. *Ecol. Lett.* **11**, 609–623 (2008).
14. Tzedakis, P. C., Lawson, I. T., Frogley, M. R., Hewitt, G. M. & Preece, R. C. Buffered tree population changes in a Quaternary refugium: evolutionary implications. *Science* **297**, 2044–2047 (2002).
15. Fordham, D. A., Saltre, F., Brown, S. C., Mellin, C. & Wigley, T. M. L. Why decadal to century timescale palaeoclimate data are needed to explain present-day patterns of biological diversity and change. *Glob. Change Biol.* **24**, 1371–1381 (2018).
16. Cooper, A. et al. Abrupt warming events drove Late Pleistocene Holarctic megafaunal turnover. *Science* **349**, 602–606 (2015).
17. Fordham, D. A., Brown, S. C., Wigley, T. M. L. & Rahbek, C. Cradles of diversity are unlikely relics of regional climate stability. *Curr. Biol.* **29**, R356–R357 (2019).
18. Wallace, A. R. *Tropical Nature, and Other Essays* (Macmillan and Company, 1878).
19. Mittermeier, R. A., Turner, W. R., Larsen, F. W., Brooks, T. M. & Gascon, C. in *Biodiversity Hotspots: Distribution and Protection of Conservation Priority Areas* (eds Zachos, F. E. & Habel, J. C.) 3–22 (Springer, 2011).
20. Connell, J. H. Diversity in tropical rain forests and coral reefs. *Science* **199**, 1302–1310 (1978).
21. Johnson, D. J., Condit, R., Hubbell, S. P. & Comita, L. S. Abiotic niche partitioning and negative density dependence drive tree seedling survival in a tropical forest. *Proc. R. Soc. B* **284**, 20172210 (2017).
22. Barlow, J. et al. The future of hyperdiverse tropical ecosystems. *Nature* **559**, 517–526 (2018).
23. Burke, K. D. et al. Pliocene and Eocene provide best analogs for near-future climates. *Proc. Natl Acad. Sci. USA* **115**, 13288 (2018).
24. Stillman, J. H. Acclimation capacity underlies susceptibility to climate change. *Science* **301**, 65–65 (2003).
25. Frieler, K. et al. Limiting global warming to 2 °C is unlikely to save most coral reefs. *Nature Clim. Change* **3**, 165–170 (2012).
26. Tewksbury, J. J., Huey, R. B. & Deutsch, C. A. Putting the heat on tropical animals. *Science* **320**, 1296–1297 (2008).
27. Sniderman, J. M. K. et al. Southern Hemisphere subtropical drying as a transient response to warming. *Nat. Clim. Change* **9**, 232–236 (2019).
28. Lohman, D. J. et al. Biogeography of the Indo-Australian archipelago. *Annu. Rev. Ecol. Evol. Syst.* **42**, 205–226 (2011).
29. Pellissier, L. et al. Quaternary coral reef refugia preserved fish diversity. *Science* **344**, 1016–1019 (2014).
30. Mora, C. et al. Biotic and human vulnerability to projected changes in ocean biogeochemistry over the 21st century. *PLoS Biol.* **11**, e1001682 (2013).

Methods

Annual-mean, gridded temperature and precipitation data were derived from 18 AOGCMs (Supplementary Table 1 and Supplementary Fig. 4) for the entire globe, simulated under preindustrial control conditions and RCPs 4.5 and 8.5[31]. Palaeoclimate simulations were derived from the Community Climate System Model v.3 TraCE-21ka simulations[32]. All data were regridded to a common 2.5° × 2.5° grid. For plotting only, all gridded results were reprojected to the Mollweide equal area projection with a grid cell resolution of 250 km.

Preindustrial control runs of varying run lengths (Supplementary Table 1) were used to estimate internally generated natural variability in near century (91 yr) global mean trends in air temperature (°C yr^{-1}) using generalized least-squares regression and maximally overlapping windows[17]. Windows were limited to 91-yr periods for past and future estimates of climate stability because the RCP scenarios only have a 91-yr period of suitable data (see Supplementary Methods for details). Trends in area-weighted global mean temperature were calculated separately for each AOGCM by using the slope of the generalized least-squares model. This information was used to generate individual-AOGCM cumulative distribution functions (CDFs; Supplementary Fig. 5). Trends were bootstrapped 1,000 times to ensure that models with longer run times did not influence the shape of the ensemble average CDF. We used the 90th percentile[33] of the ensemble average preindustrial control CDF to calculate a threshold for identifying periods with the highest trends in global mean temperature under naturally varying climatic conditions.

We used an identical approach, without the bootstrap, to calculate past trends (using the TraCE-21ka annual palaeoclimate simulations) during the late Quaternary period before industrialization (21,000 yr BP to 100 yr BP). We applied the upper trend threshold from the preindustrial control runs to the palaeoclimate trends to identify specific periods of rapid change in global mean temperature during the late Quaternary (Supplementary Fig. 6). The time series of palaeoclimate simulations was then subset on the basis of these periods of rapid change in global mean temperature[17]. In doing so, local measures of trend and variability (that is, at the grid cell) were constrained to centuries of unusually high trends in global mean temperature (that is, periods of rapid changes in global mean temperature).

Generalized least-squares regression was used to calculate trend and variability (s.d. of residuals from the trends) in annual temperature and precipitation at the grid-cell level for the subset of palaeoclimate simulations (periods of rapid change in global temperature) and multimodel-averaged twenty-first-century projections for RCPs 4.5 and 8.5. Climate regimes were then defined categorically at a grid-cell level as either stable or unstable, where 'stable' required both the centennial trend and variability of the particular variable (temperature or precipitation) to be less than or equal to the 50th percentile of the corresponding global mean CDF (calculated separately for terrestrial and oceanic realms) and unstable otherwise; precipitation analysis was constrained to the terrestrial realm only. We also identified very stable and very unstable climatic regions using the 25th and 75th percentiles for trend and variability, respectively. If both the trend and s.d. were less than or equal to the 25th percentile then the cell was considered stable (P_{25}), whereas it was considered unstable if both were greater than or equal to the 75th percentile (P_{75}). Where trend and variability fell between the 25th and 75th percentile, the median was used as a breakpoint to identify low or high trend and variability. Sensitivity analysis[17] has shown that the timing and location of areas of climate stability are insensitive to variation (±10%) in the cut-off points used. The thresholds for categorical analysis such as these are, to some extent, affected by the cumulative distribution function of the entire dataset. Hence, we recommend that all categorical results be interpreted in combination with SNR results.

We used generalized additive models[34]—fitted with a negative binomial distribution and log link[35]—and multimodel inference[36] to determine the relationship between species richness and trend and variability in past temperature and precipitation. Species richness was estimated at a grid-cell level for three classes of animals (amphibians, birds, mammals) following Holt et al.[37]. Some of the statistical models also used location (latitude and longitude) as predictor variables. Our measure of species richness is likely to be weighted towards wide-ranging species[38]. Furthermore, our analysis of the role of past climate stability on species richness does not consider contemporary climate and environmental disturbance, and their potential to be spatially correlated with late Quaternary climate change[7].

We calculated SNRs by dividing the trend by the variability (s.d. of residuals about the local trend) for each grid cell for each near century of rapid change in the global mean temperature and then calculated the median values. We quantified the shift in SNR between the past and the future (ΔSNR = SNR Future − SNR Past) for five latitudinal bands: High North (50°N to 90°N), High South (90°S to 50°S), Mid North (20°N to 50°N), Mid South (50°S to 20°S) and the Tropics (20°S to 20°N). To determine whether changes between past and future SNR in Wallace Zoogeographic regions[37] ($n = 19$) were statistically different, we scaled values in each region across time (to between 0 and 1) and used Kernel densities (KDs) to calculate the amount of overlap in their distributions. A Kolmogorov–Smirnov test was used to assess the statistical significance of the differences in the shape, spread and median Kernal density values (see the Supplementary Information for an extended description of the methods).

Reporting Summary. Further information on research design is available in the Nature Research Reporting Summary linked to this article.

Data availability

The source data used for the analysis of preindustrial control and future RCP scenarios are available through the Earth System Grid Federation data portals (for example, https://esgf-node.llnl.gov/projects/esgf-llnl/) with scripts to download the data available at https://github.com/GlobalEcologyLab/ESGF_ClimateDownloads. Data used for the analysis of climates from the LGM to preindustrialization are available through the PaleoView software (https://github.com/GlobalEcologyLab/PaleoView). Data used to recreate the figures is available from the corresponding authors on request.

Code availability

The code used to generate the outputs (trends, variability, SNR) is available from the corresponding authors on request.

References

31. van Vuuren, D. P. et al. The representative concentration pathways: an overview. *Climatic Change* **109**, 5–31 (2011).
32. Liu, Z. et al. Transient simulation of last deglaciation with a new mechanism for Bolling–Allerod warming. *Science* **325**, 310–314 (2009).
33. Zhang, X. et al. Indices for monitoring changes in extremes based on daily temperature and precipitation data. *WIREs Clim. Change* **2**, 851–870 (2011).
34. Wood, S. N. *Generalized Additive Models: An Introduction with R* (Chapman and Hall/CRC, 2017).
35. Ver Hoef, J. M. & Boveng, P. L. Quasi-poisson vs. negative binomial regression: how should we model overdispersed count data? *Ecology* **88**, 2766–2772 (2007).
36. Grueber, C. E., Nakagawa, S., Laws, R. J. & Jamieson, I. G. Multimodel inference in ecology and evolution: challenges and solutions. *J. Evol. Biol.* **24**, 699–711 (2011).
37. Holt, B. G. et al. An update of wallace's zoogeographic regions of the world. *Science* **339**, 74–78 (2013).
38. Jetz, W. & Rahbek, C. Geographic range size and determinants of avian species richness. *Science* **297**, 1548–1551 (2002).

Acknowledgements

This research was funded by an Australian Research Council Future Fellowships awarded to D.A.F. (grant no. FT140101192) and a Discovery Grant (grant no. DP130103261) awarded to T.M.L.W.

Author contributions

D.A.F conceived and led the project. S.C.B and T.M.L.W. did the analysis. B.L.O.-B. and C.R. guided the analysis of climate and macroecological datasets. S.C.B drafted the manuscript and all authors commented on the paper.

Competing interests

The authors declare no competing interests.

Additional information

Extended data is available for this paper at https://doi.org/10.1038/s41558-019-0682-7.

Supplementary information is available for this paper at https://doi.org/10.1038/s41558-019-0682-7.

Correspondence and requests for materials should be addressed to S.C.B. or D.A.F.

Peer review information *Nature Climate Change* thanks Glenn Yannic and the other, anonymous, reviewer(s) for their contribution to the peer review of this work.

Reprints and permissions information is available at www.nature.com/reprints.

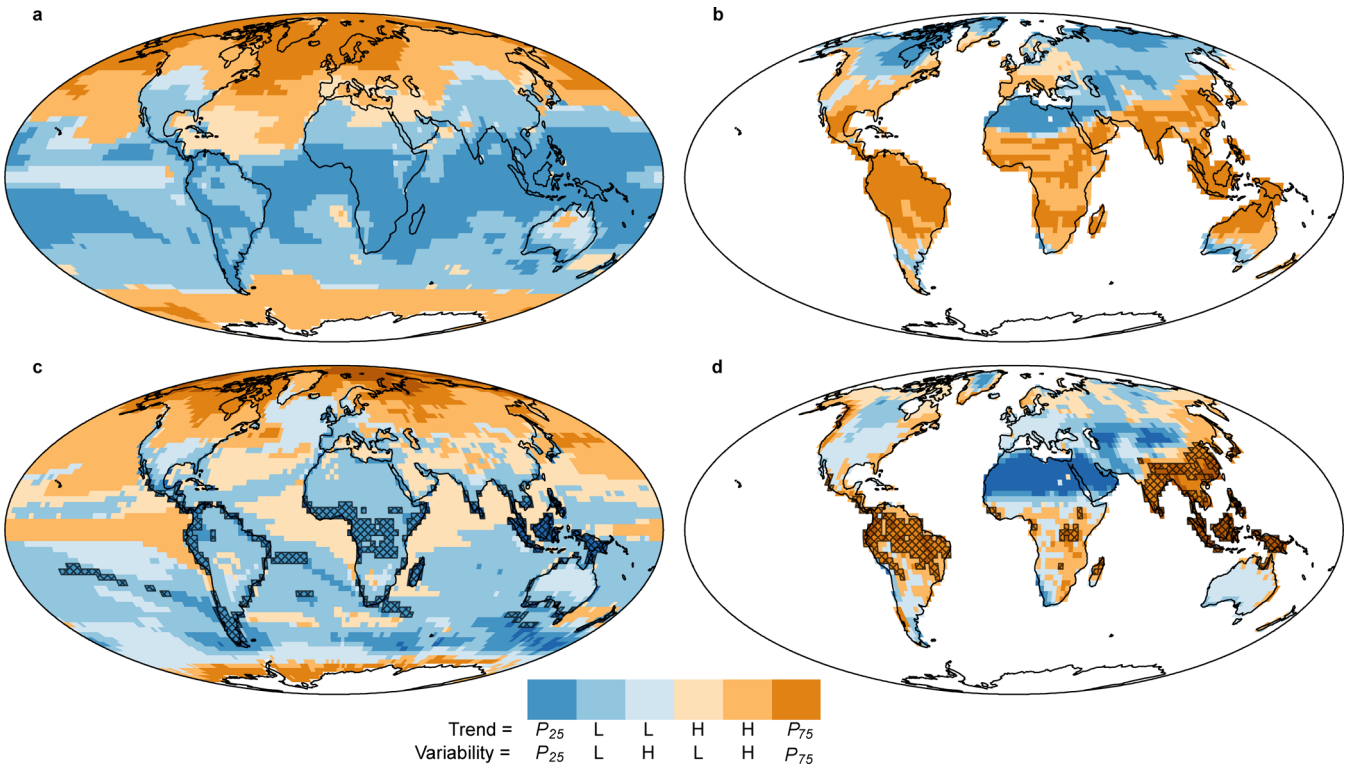

Extended Data Fig. 1 | Classified median trend and variability during periods of rapid change in global mean temperature. Panels show the past (**a**, **b**) and the future for RCP 4.5 (**c**, **d**) for surface temperature (**a**, **c**) and precipitation (**b**, **d**). The six classes map median trend and variability (s.d. of residuals from the trend) calculated separately for land and ocean: ≤ 25th (P25); > 25th and ≤ 50th (Low-Low); ≤ 50th for trend and ≥ 50th for variability (Low-High); > 50th for trend and ≤ 50th for variability (High-Low); > 50th and ≤ 75th (High-High); > 75th (P75). The hatched overlays in **c** and **d** show climatic conditions that are considered as either stable (≤ P25, surface temperature) or unstable (≥ P75, precipitation) at a global scale in both the past and future.

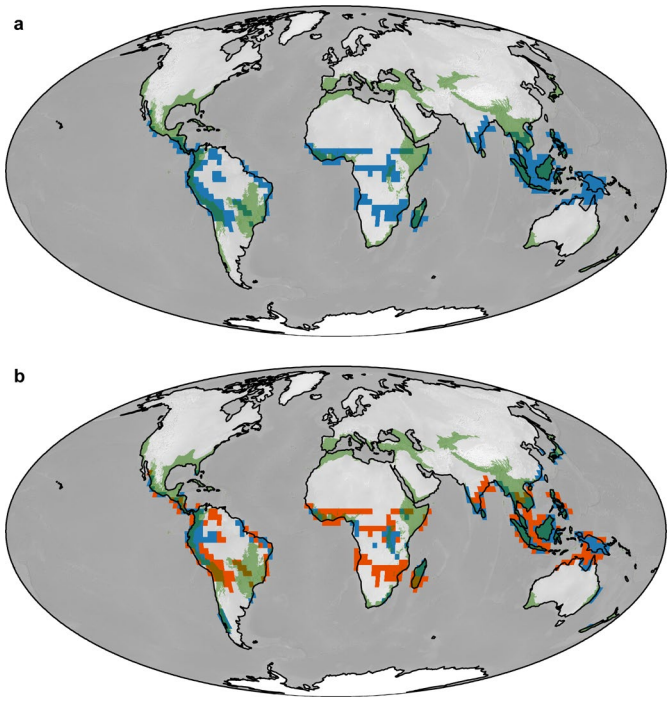

Extended Data Fig. 2 | Areas of overlap in stable surface temperature (≤ 25th percentile) and unstable precipitation (≥ 75th percentile) conditions over land. Panels show the past (**a**), and the future under RCP 4.5 (**b**). Areas of overlap - regions where climate conditions are hypothesized to drive higher contemporary species richness – are shown in blue. Areas in orange in **b**, show differences between the past and the future (i.e., areas of overlap that are lost). The transparent green regions overlaid on the maps are biodiversity hotspots[19].

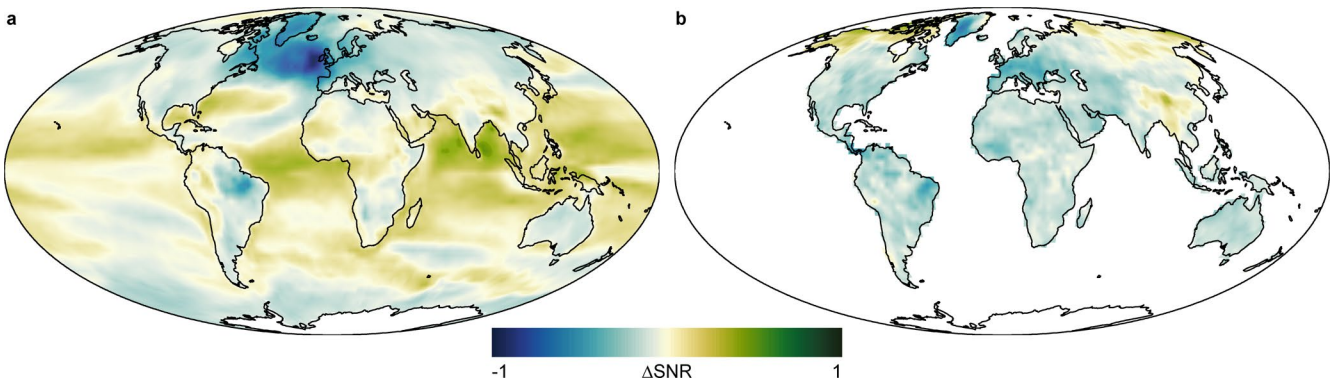

Extended Data Fig. 3 | Comparison of past and future signal-to-noise ratios. Grid cell differences (ΔSNR) in signal-to-noise ratio (SNR = trend/variability) for centuries of rapid change in global-mean temperature since 21,000 BP and for RCP 4.5 calculated for air temperature (**a**) and precipitation (**b**).

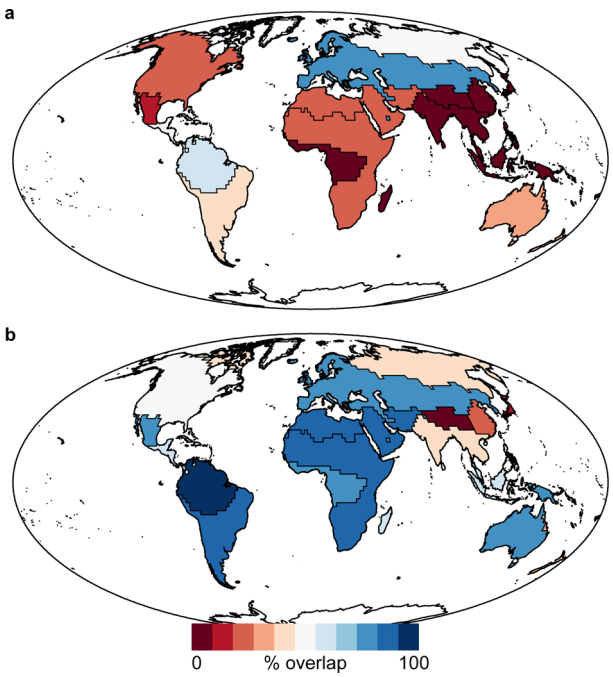

Extended Data Fig. 4 | Regional changes in SNR for Wallace Zoogeographic regions. Map of percent overlap between empirical kernel density estimates (KDE) for temperature SNR (**a**) and precipitation SNR (**b**) calculated during past rapid shifts in global-mean temperature and under an RCP 4.5 scenario.

nature research

Corresponding author(s): Stuart C Brown, Damien A Fordham

Last updated by author(s): Dec 2, 2019

Reporting Summary

Nature Research wishes to improve the reproducibility of the work that we publish. This form provides structure for consistency and transparency in reporting. For further information on Nature Research policies, see Authors & Referees and the Editorial Policy Checklist.

Statistics

For all statistical analyses, confirm that the following items are present in the figure legend, table legend, main text, or Methods section.

n/a	Confirmed
☐	☒ The exact sample size (*n*) for each experimental group/condition, given as a discrete number and unit of measurement
☐	☒ A statement on whether measurements were taken from distinct samples or whether the same sample was measured repeatedly
☐	☒ The statistical test(s) used AND whether they are one- or two-sided *Only common tests should be described solely by name; describe more complex techniques in the Methods section.*
☐	☒ A description of all covariates tested
☐	☒ A description of any assumptions or corrections, such as tests of normality and adjustment for multiple comparisons
☐	☒ A full description of the statistical parameters including central tendency (e.g. means) or other basic estimates (e.g. regression coefficient) AND variation (e.g. standard deviation) or associated estimates of uncertainty (e.g. confidence intervals)
☐	☒ For null hypothesis testing, the test statistic (e.g. *F*, *t*, *r*) with confidence intervals, effect sizes, degrees of freedom and *P* value noted *Give P values as exact values whenever suitable.*
☒	☐ For Bayesian analysis, information on the choice of priors and Markov chain Monte Carlo settings
☒	☐ For hierarchical and complex designs, identification of the appropriate level for tests and full reporting of outcomes
☐	☒ Estimates of effect sizes (e.g. Cohen's *d*, Pearson's *r*), indicating how they were calculated

Our web collection on statistics for biologists contains articles on many of the points above.

Software and code

Policy information about availability of computer code

Data collection	No software was used in the data collection process of this work.
Data analysis	Data analysis was performed in R (version 3.5.1) using the standard base R packages and the following packages: doParallel, dplyr, ncdf4, nlme, raster. Code is available on reasonable request from the corresponding authors (SCB, DAF)

For manuscripts utilizing custom algorithms or software that are central to the research but not yet described in published literature, software must be made available to editors/reviewers. We strongly encourage code deposition in a community repository (e.g. GitHub). See the Nature Research guidelines for submitting code & software for further information.

Data

Policy information about availability of data

All manuscripts must include a data availability statement. This statement should provide the following information, where applicable:

- Accession codes, unique identifiers, or web links for publicly available datasets
- A list of figures that have associated raw data
- A description of any restrictions on data availability

The source data used for the analysis of pre-industrial control and future RCP scenarios is available through the Earth System Grid Federation data portals (e.g. https://esgf-node.llnl.gov/projects/esgf-llnl/) with scripts to download the data available at https://github.com/GlobalEcologyLab/ESGF_ClimateDownloads. Data used for the analysis of climates from the last glacial maximum to pre-industrialisation is available through the PaleoView software (https://github.com/GlobalEcologyLab/PaleoView). Data used to recreate the figures is available from the corresponding authors on request.

Field-specific reporting

Please select the one below that is the best fit for your research. If you are not sure, read the appropriate sections before making your selection.

☐ Life sciences ☐ Behavioural & social sciences ☒ Ecological, evolutionary & environmental sciences

For a reference copy of the document with all sections, see nature.com/documents/nr-reporting-summary-flat.pdf

Ecological, evolutionary & environmental sciences study design

All studies must disclose on these points even when the disclosure is negative.

Study description	We generated near-century measures of trend, variability, and signal-to-noise ratios (SNR) in temperature and precipitation for periods of extreme global change during the Quaternary. These measures were linked to contemporary patterns of species richness, and compared with projected patterns of climate change to estimate impacts of anthropogenic climate change on biodiversity hotspots and species richness patterns.
Research sample	Temperature and precipitation data for 18 atmosphere ocean global circulation models (AOGCM) during pre-industrial conditions and two future climate scenarios (RCP 4.5 and RCP 8.5) were extracted from Earth System Grid Federation (ESGF) data portals. The 18 models from the ESGF portals were analysed independently with the estimated trends, variability, and SNR combined to produce a multi-model ensemble average within each scenario to account for inter- and intra-model biases. Estimates of paleo temperature and precipitation were extracted from TraCE-21ka simulations preprocessed for PaleoView software. Species richness maps were produced from IUCN range maps for birds, amphibians, and mammals following Holt et al (2013; doi:10.1126/science.1228282). We used the 90th percentile of a CDF built on the temperature trends from the ensemble average pre-industrial control to determine a threshold for identifying periods with the highest trends in global-mean temperature under "naturally" varying climatic conditions. The time series of paleoclimate simulations was then subset to periods that exceeded this threshold to identify periods of rapid change in global-mean temperature between 21,000 and 100BP.
Sampling strategy	Sample sizes were chosen based on the number of grid cells covering the globe at 2.5° resolution (n=10,368). Sample sizes for species richness data were based on upscaling the data from it's native resolution to 2.5° and excluding cells where NA values occurred for temperature or precipitation (e.g. precipitation or temperature over the ocean)
Data collection	Modelled climate data was extracted from ESGF data portals and PaleoView software. Holt et al. (2013; doi:10.1126/science.1228282) collected the species distribution data.
Timing and spatial scale	Global gridded yearly temperature and precipitation data between 21,000BP and 100BP, and from 2010-2100 AD.
Data exclusions	Precipitation data was excluded from oceanic realms (n=6,302 grid-cells) as it was not considered relevant to the study. Paleo temperature and precipitation data that did not occur during periods of extreme global change was excluded from median estimates of trend, variability, and SNR for both variables.
Reproducibility	Code for the analysis was written in R and is available on request for reproducibility. There was no attempt to repeat the analysis.
Randomization	Based on location cells were assigned to corresponding latitudinal bands and Wallace Zoogeographic regions (doi:10.1126/science.1228282) for some analyses
Blinding	Blinding to was not relevant to this study

Did the study involve field work? ☐ Yes ☒ No

Reporting for specific materials, systems and methods

We require information from authors about some types of materials, experimental systems and methods used in many studies. Here, indicate whether each material, system or method listed is relevant to your study. If you are not sure if a list item applies to your research, read the appropriate section before selecting a response.

Materials & experimental systems

n/a	Involved in the study
☒	☐ Antibodies
☒	☐ Eukaryotic cell lines
☒	☐ Palaeontology
☒	☐ Animals and other organisms
☒	☐ Human research participants
☒	☐ Clinical data

Methods

n/a	Involved in the study
☒	☐ ChIP-seq
☒	☐ Flow cytometry
☒	☐ MRI-based neuroimaging